IEEE Access
Multidisciplinary | Rapid Review | Open Access Journal

Received October 20, 2017, accepted December 14, 2017, date of publication December 27, 2017,
date of current version February 14, 2018.

Digital Object Identifier 10.1109/ACCESS.2017.2787663

Research on Robust Model Predictive Control for Electro-Hydraulic Servo Active Suspension Systems

DAZHUANG WANG[1], DINGXUAN ZHAO[2], MINGDE GONG[2], AND BIN YANG[1]
[1]School of Mechanical Science and Engineering, Jilin University, Changchun 130022, China
[2]School of Mechanical Engineering, Yanshan University, Qinhuangdao 066004, China

Corresponding author: Dingxuan Zhao (zdx@ysu.edu.cn)

This work was supported by the National Key R&D Program of China under Grant 2016YFC0802902. This work was recommended by ICACMVE 2017.

ABSTRACT The suspension system is an important component of any vehicle as it transmits the force and torque between the wheel and the frame, satisfying the requirements of ride comfort and handling stability. To solve the problem of active suspension control, a seven-degree-of-freedom active suspension system model with electrohydraulic actuators is established. Through the approximate expansion in the rolling time domain, a robust model predictive controller (RMPC) for the active suspension system is designed and the RMPC of the active suspension is deduced by defining the RMPC performance evaluation function. A fractional PID controller is used to control the active suspension hydraulic actuators. The accuracy and efficiency of the controller are verified with prototype vehicle simulations and road experiments. Results show that the performance of the active suspension system is better than that of traditional suspension systems. The ride comfort and handling stability are considerably improved by the reductions of vertical acceleration, pitch angle, and roll angle accelerations.

INDEX TERMS Active suspension, approximate expansion, model predictive control, fractional PID, road experiment.

I. INTRODUCTION

The suspension system is an important component of a vehicle. The elastic connection between the suspension axle and the vehicle body can transmit the force and torque between the wheel and the frame, thereby improving vehicle comfort and ensuring vehicle handling stability. With the development of the automobile industry and the advancements in related technologies, the demand for improving the performance of automobiles has also increases, especially in terms of improving the vibration of automobiles.

Suspensions have three classifications: passive, semi-active, and active suspension. Although passive suspension is extensively used as the traditional suspension system of the mechanical structure, it cannot simultaneously address ride comfort and handling stability. Semi-active suspension can be adjusted by single parameter variables (e.g., elastic or damping elements), which can partly replace the active suspension function. Active suspension can adjust the body posture and the suspension damping performance through active controllable actuators in accordance with road conditions and control laws to maximize the entire vehicle performance.

The active suspension system includes an actuator and a matching sensor and control unit, which can input force and displacement to the suspension system based on the passive suspension system. In the control process, the active suspension system adjusts the output of the active suspension actuator according to the real-time changes in road input and the vehicle status, thereby canceling the influence of the road and obtaining a good shock absorption effect while controlling the height and attitude.

Many control methods have been previously applied to the active suspension control [1]–[5], because active suspension can satisfy the ride comfort and handling stability requirements. For example, Li *et al.* [6] designed an adaptive sliding-mode control for nonlinear active suspension systems, including varying masses and actuator nonlinearity, and used

the Takagi-Surgeon (T-S) fuzzy approach to describe the uncertainties. Brezas and Smith [7] modeled a time-domain optimal control using quarter-car and full-car models of active suspensions, which they generalized by incorporating road disturbances and a representation of driver inputs and considering this factor in the state estimation; they also considered the performance index as a risk-sensitive LQG criterion. Pan *et al.* [8] investigated the problem of finite-time stabilization for vehicle suspension systems with hard constraints and designed a new class of continuous terminal sliding-mode control strategy for the trajectory tracking of active suspensions. Deshpande *et al.* [9] established a dual-objective nonlinear controller for the active suspension system to provide ride comfort and keep the suspension deflection within the constraint; they analyzed the control scheme and assessed for large classes of road profiles through simulation and experiment. In [10], an output feedback active controller that uses a recursive derivative nonsingular higher order terminal sliding mode is proposed for the active suspension system with nonlinearities, external disturbances, and uncertainties to achieve ride comfort while maintaining road holding.

Although variable control methods were used in the active suspension system, the full-vehicle control effect was not considered in some papers, and the interaction among the four active suspensions was ignored [1], [3], [6]. In addition, the actuator is considered an ideal power output unit in several active suspension control methods [2], [4], [7], which disregard the practical application. Meanwhile, because the active suspension system and hydraulic actuators have high nonlinear and uncertain factors, it also suffers from the traditional controller effect.

Model predictive control (MPC) is an optimal control proposed in the 1970s to address the increasing control requirements [11]. With the development of industrial technology, the accurate mathematical model of the multi-variable and multi-dimension load system in the industrial process is difficult to suggest. At the same time, the MPC has also been widely studied and applied due to the following advantages: a low demand for system modeling, the rolling optimization strategy has a good dynamic control effect, and feedback correction is helpful for improving the robustness of the control system. With in-depth study, MPC has been widely used in solving nonlinear problems [12], [13] and in investigating input and output constraints systems [14], [15]. For example, in [16], two model predictive controllers were designed for active suspension systems with the road height profile in front of the car measured by vehicle sensors. The results of that study showed that preview active suspension control significantly improved ride comfort if the oncoming road height profile is measured using vehicle sensors. Cheng *et al.* [17] presented a design for a nonlinear model predictive control (NMPC) to solve the displacement tracking problem of piezoelectric actuators, which have been widely used in Nano-technology. In that study, the tracking control problem is converted into an optimization problem by the principle of NMPC, and the most distinguished feature of the proposed approach is that the inversion model of hysteresis is no longer required; thereby avoiding the inversion-imprecision problem encountered in the widely used inversion-based control algorithms. Hu *et al.* [18] established a multiplexed model predictive control (MMPC), which can effectively reduce the computational burden of online optimization, using soft constraints. The results showed that the performance of vehicles can be improved significantly. Schnelle and Eberhard [19] presented an adaptive NMPC for the trajectory tracking of flexible-link manipulators using the unscented Kalman filter in the optimization of the adaptability of the problem at each time step; the prediction and input actions were effectively improved, and a detailed fuzzy arithmetic analysis was carried out to quantify the effects on the control structure of the uncertainties and to obtain a robustness assessment. Lopez-Sanz *et al.* [13] used the NMPC, a powerful controller for achieving multiple objectives in multiple input–multiple output systems, for the thermal management of plug-in hybrid electric vehicles, while obtaining a better control effect. The developed model and optimization formula allowed for direct improvements to enable the easy implementation of NMPC in other cooling circuit architectures.

MPC has low requirements on the model and can successfully overcome the shortcomings of modern control theory model. MPC draws from the idea of optimal control and uses scrolling finite-period optimization instead of invariant global optimization. The active suspension system, with uncertain factors and input–output constraints, can be solved through the model predictive control.

This paper consists of seven sections. In Section 1, the active suspension system and available control methods are introduced, the shortcomings of several control methods are considered in practical application, and the MPC is proposed. Section 2 presents the modeling of the active suspension system. First, considering the interaction between the four vehicle suspensions, the seven degree-of-freedom model of vehicle active suspension is established, and the model of valve controlled asymmetrical hydraulic cylinder is considered to increase the actual application effect of the model. Finally, a random road input model is developed and combined with the vehicle model to obtain the control model. In Sections 3–4, the designs of the active suspension model predictive controller and the fractional order PID controller of the hydraulic actuators are presented, respectively. Section 5 discusses the simulation of the designed controller and the results. In Section 6 discusses the road experiment of the prototype vehicle, which is carried out to verify the validity of the designed controllers. Section 7 presents the conclusion. The simulation and experimental results indicate that, compared with the passive suspension system, the proposed active suspension system can effectively reduce the vertical acceleration, pitch, and roll angle accelerations of vehicles, while increasing the vehicle handling stability and ride comfort.

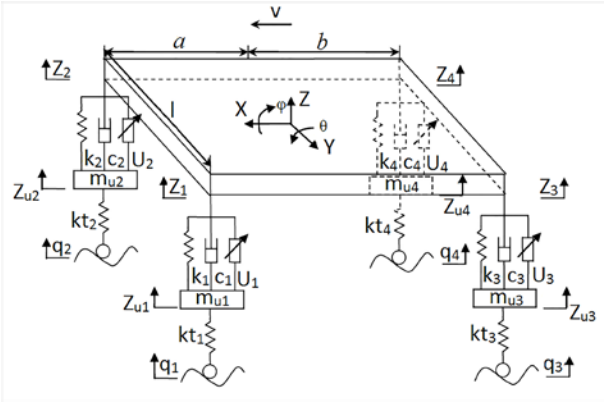

FIGURE 1. 7-DOF model of active suspension system.

II. ACTIVE SUSPENSION SYSTEM DYNAMICS

A. THE SEVEN-DEGREE-OF-FREEDOM ACTIVE SUSPENSION SYSTEM MODEL

The seven-degree-of-freedom automotive active suspension system model is shown in Fig.1, which consists of four vertical unsprung masses and the degrees of freedom due to pitch, roll, and vertical motion of the mass center [20]. The variables of the active suspension model are shown in Table 1.

TABLE 1. Variables of active suspension model (i = 1, 2, 3, 4).

Symbol	Quantity
m	mass of the vehicle body
mui	unsprung masses
z	displacement of the vehicle body
zi	displacements between vehicle body and suspensions
zui	unsprung mass displacements
qi	road displacements
a	distance between center of mass and front suspension
b	distance between center of mass and rear suspension
θ	pitch angle of the vehicle body
φ	roll angle of the vehicle body
Jx	moment of inertia of the X axis
Jy	moment of inertia of the Y axis
ki	stiffness coefficients of the springs
kti	stiffness coefficients of the tires
ci	damping coefficients
Ui	forces generated by actuators

According to Newton's second law, we can obtain the vertical motion of the body centroid, body pitching, and roll rotation equations as follows:

$$\left.\begin{aligned} m\ddot{z} &= -F_1 - F_2 - F_3 - F_4 \\ J_y\ddot{\theta} &= a\left(F_1 + F_2\right) - b\left(F_3 + F_4\right) \\ J_x\ddot{\varphi} &= \tfrac{l}{2}\left(-F_1 + F_2 - F_3 + F_4\right) \end{aligned}\right\}. \tag{1}$$

In the preceding equations, the Fi (i = 1,2,3,4) acts as the force between the suspension and the vertical body:

$$F_i = k_i\left(z_i - z_{ui}\right) + c_i\left(\dot{z}_i - \dot{z}_{ui}\right) - U_i. \tag{2}$$

The dynamic equation of the vertical motion of unsprung mass is

$$m_{ui}\ddot{z}_{ui} = k_i(z_i - z_{ui}) + c_i(\dot{z}_i - \dot{z}_{ui}) - k_{ti}(z_{ui} - q_i) - U_i. \tag{3}$$

According to the spatial motion law of the rigid body, the dynamic relationship among the four suspension systems, the body connection points, the body centroid vertical movement, the pitching rotation, and the roll rotation can be demonstrated as:

$$\begin{cases} z_1 = z - a\sin\theta + \dfrac{l}{2}\sin\varphi \\ z_2 = z - a\sin\theta - \dfrac{l}{2}\sin\varphi \\ z_3 = z + b\sin\theta + \dfrac{l}{2}\sin\varphi \\ z_4 = z + b\sin\theta - \dfrac{l}{2}\sin\varphi. \end{cases} \tag{4}$$

As a rigid body structure, the pitch and roll angles of the vertical body assume change in a small angle range. Set the following equations:

$$\theta \approx \sin\theta, \quad \varphi \approx \sin\varphi. \tag{5}$$

Establish the state equation and define the system state variable X as:

$$X = \begin{bmatrix} z & \theta & \varphi & z_{u1} & z_{u2} & z_{u3} & z_{u4} \\ \dot{z} & \dot{\theta} & \dot{\varphi} & \dot{z}_{u1} & \dot{z}_{u2} & \dot{z}_{u3} & \dot{z}_{u4} \end{bmatrix}^T.$$

The active suspension system can be expressed in the following state equation:

$$\dot{X} = AX + BU + EQ, \tag{6}$$

where U is the control vector which represents the output force of the EH servo actuator of each suspension subsystem, Q is the road input vector of four tires, and A, B, and E are divided into coefficient matrixes.

System output Y is defined as:

$$Y = \begin{bmatrix} \ddot{z} & \ddot{\theta} & \ddot{\varphi} & z_1 - z_{u1} & z_2 - z_{u2} & z_3 - z_{u3} & z_4 - z_{u4} \end{bmatrix}^T.$$

The output equation of the system is:

$$Y = CX + DQ, \tag{7}$$

where C and D are coefficient matrixes.

B. THE VALVE-CONTROLLED CYLINDER MODEL

In this study, the active suspension actuator is the asymmetric cylinder, which is controlled by the EH servo valve. The valve-controlled cylinder model is shown in Fig. 2, and the variables are shown in Table 2 [21].

The dynamic equation of the hydraulic actuator is expressed as [22]

$$\frac{V_t}{4\beta_e}\dot{P}_L = Q_L - C_{tm}P_L - A_p\left(\dot{z}_s - \dot{z}_u\right), \tag{8}$$

where

$$Q_L = C_d\omega x_v\sqrt{\frac{P_s - \mathrm{sgn}\left(x_v\right)P_L}{\rho}}.$$

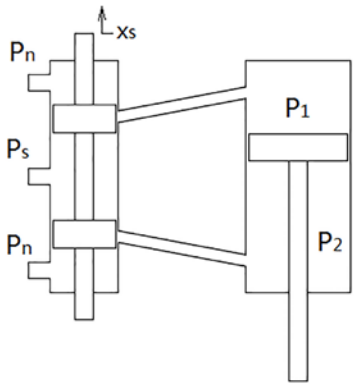

FIGURE 2. Model of non-symmetrical cylinder.

TABLE 2. Variables of non-symmetrical cylinder model (i = 1, 2, 3, 4).

Symbol	Quantity
P_s	supply pressure
P_n	return pressure
P_1	pressures in the upper cylinder
P_2	pressures in the lower cylinder
A_p	piston area
x_s	spool valve displacement
i_s	valve current
τ	mechanical time constant
βe	bulk modulus of hydraulic fluid
V_t	total volume of actuator cylinder chamber
C_t	leakage coefficient
C_d	discharge coefficient
ρ	density of hydraulic fluid
w	spool valve area gradient

The dynamic equation of the hydraulic actuator [23] is expressed as

$$\dot{U} = -\alpha A_p^2 (\dot{z}_s - \dot{z}_u) - \beta U + \omega A_P x_{sp} \sqrt{P_s - \mathrm{sgn}(x_s)\, U/A_p}. \tag{9}$$

The servo valve system is given by

$$\dot{x}_s = (-x_s + i_s)/\tau. \tag{10}$$

Among them,

$$\alpha = 4\beta_e/V_t, \quad \beta = \alpha C_t, \ \omega = \alpha C_d w \sqrt{1/\rho}.$$

C. THE RANDOM ROAD INPUT MODEL

If we ignore the vibration generated with the power and transmission systems of a vehicle, the unevenness of the road surface becomes the most important factor affecting vehicle ride comfort. The model of random road surface is a continuous random excitation, which is the most common model employed in simulation and practical applications with the goal of obtaining more representative experimental data. To study and simulate the active suspension control strategy, the time domain model of road input is established.

When the vehicle travels at a speed (v), the time frequency (f) represents the number of waves contained in a time unit and is the product of the space frequency and the velocity

$$f = v \cdot n. \tag{11}$$

The power spectral density of road roughness is given by

$$G_q(f) = \frac{1}{v} G_q(n), \tag{12}$$

where $G_q(n_0)$ is the road roughness coefficient expressed as

$$\mathrm{G}_q(n) = \mathrm{G}_q(n_0) \left(\frac{n}{n_0}\right)^{-w}.$$

When $w = 2$,

$$G_q(f) = G_q(n_0)\, n_0^2 \frac{v}{f^2}, \tag{13}$$

where n_0 indicates the standard spatial frequency.

Let $W(t)$ be the white noise signal. The pavement contour function is obtained by passing the low-pass filter with function H. Then, the transfer function is

$$H(jw) = \frac{2\pi n_0 \sqrt{G_q(n_0)\, v}}{jw + w_0}. \tag{14}$$

We can obtain the following stochastic pavement model:

$$\dot{q}(t) = -2\pi f_0 v q(t) + 2\pi \mathrm{n}_0 \sqrt{\mathrm{G}_q(n_0)\, v} w(t), \tag{15}$$

where f_0 is the road spatial cutoff frequency.

III. MODEL PREDICTIVE CONTROL

Before designing the controller, the following assumptions are made: the active suspension system is dynamically stable, the output and the reference signal can be continuously differentiable for time t [24], and the origin is the system balance point.

The calculation is simplified as follows:

$$\frac{\partial CX}{\partial x}\dot{x} = L_C, \quad \frac{\partial BU}{\partial u}\dot{u} = L_U.$$

The derivative of the system output Y is given by:

$$\begin{aligned}
\dot{y} &= \frac{\partial CX}{\partial x}\dot{x} = L_C \\
&\cdots, \\
y^{(\rho+2)} &= \frac{\partial L_C^{(\rho+1)}}{\partial x}\dot{x} + \frac{\partial L_C^{(\rho+1)}}{\partial u}\dot{u} + \frac{\partial L_U L_C^{(\rho)}}{\partial x}\dot{x}\dot{u} \\
&\quad + \frac{\partial L_U L_C^{(\rho)}}{\partial u}\dot{u}^2 + L_U L_C \rho \ddot{u} \\
&= L_C \rho + 2 + L_U L_C \rho \ddot{u} + P_1(x, u, \dot{u}),
\end{aligned}$$

where:

$$\begin{aligned}
P_1(x, u, \dot{u}) = &\frac{\partial L_C^{(\rho+1)}}{\partial u}\dot{u} + \frac{\partial L_U L_C^{(\rho)}}{\partial x}\dot{x}\dot{u} \\
&+ \frac{\partial L_U L_C^{(\rho)}}{\partial u}\dot{u}^2 + \frac{\partial N_B^{(\rho+1)}}{\partial u}\dot{u}.
\end{aligned}$$

Repeat these steps:

$$y^{(n)} = L_C^{(n)} + L_U L_C^{(\rho)} u^{(n-\rho)} + P_{n-\rho-1}\left(x, u, \dot{u} \ldots, u^{n-\rho-1}\right). \tag{16}$$

In the rolling horizon, the output can be approximately represented as:

$$y(t+\tau) = \begin{bmatrix} y_1(t+\tau) \\ y_2(t+\tau) \\ \vdots \\ y_n(t+\tau) \end{bmatrix} = \begin{bmatrix} T_\rho(\tau) & T_n(\tau) \end{bmatrix} \overline{Y}(t), \quad (17)$$

where:

$$T_\rho(\tau) = \begin{bmatrix} I & \overline{\tau} & \cdots & \dfrac{\overline{\tau}^{(\rho-1)}}{(\rho-1)!} \end{bmatrix},$$

$$T_n(\tau) = \begin{bmatrix} \dfrac{\overline{\tau}^{(\rho)}}{\rho!} & \cdots & \dfrac{\overline{\tau}^{(\rho+n)}}{(\rho+n)!} \end{bmatrix},$$

$$\overline{Y}(t) = \begin{bmatrix} \overline{Y}_\rho(t) \\ \overline{Y}_n(t) \end{bmatrix}, \quad \overline{Y}_\rho(t) = \begin{bmatrix} Y_1(t) \\ \vdots \\ Y_m(t) \\ Y_1(t) \\ \vdots \\ Y_m^{(\rho-1)}(t) \end{bmatrix},$$

$$\overline{Y}_n(t) = \begin{bmatrix} Y_1^{(\rho)}(t) \\ \vdots \\ Y_m^{(\rho)}(t) \\ Y_1^{(\rho+1)}(t) \\ \vdots \\ Y_m^{(\rho-n)}(t) \end{bmatrix},$$

$$m = 1, 2, 3.$$

The definition of the predictive control performance index of the active suspension system is as follows:

$$minJ = \frac{1}{2}\left[y^T(t+\tau)\, Iy(t+\tau) + u^T(t+\tau)\, Ru(t+\tau)\right], \quad (18)$$

where I and R are the weight matrixes.

The optimal controller is obtained by optimizing the performance index function, and only the optimal control of the current time is selected for the actual control.

The preceding predictive control performance index (18) described can be transformed as follows

$$J = \frac{1}{2}\left[y^T(t+\tau)\, Iy(t+\tau) + u^T(t+\tau)\, Ru(t+\tau)\right]. \quad (19)$$

The necessary condition for predictive control of U is [25], [26]:

$$\frac{\partial J}{\partial u} = 0. \quad (20)$$

For the active suspension system (6–7), if the control law is taken as (21), then the performance index (18) of the closed-loop system is optimized:

$$U_m = -R^{-1}\left[\frac{\partial y^T(t+\tau)}{\partial u} Iy(t+\tau)\right]. \quad (21)$$

Considering the system in the rolling time domain, $P_{n-\rho-1}$ contains the multi-order complex nonlinear terms of x and u which affects the performance of the control system. In this paper, the $P_{n-\rho-1}$ is approximated by fuzzy logic systems (FLS), and the adaptive control is adopted to increase the robustness of the system. According to [27] and [28], FLS using IF–THEN rules, consists of the knowledge base, fuzzifier, fuzzy inference engine, fuzzy rules, and defuzzifier. The i th fuzzy IF–THEN rule can be written as

$$\mathrm{R_i}: \; If\ x_1\ is\ A_1^i\ and\ \ldots\ and\ x_n\ is\ A_n^i,$$
$$then\ y\ is\ B^i,$$

where x_i and y are the FLS input and output, $A_{i1} \ldots A_{in}$ and B^i are fuzzy sets, respectively. Fuzzy sets are associated with the fuzzy membership functions. Accordingly, FLS can be expressed as

$$Y(x) = \frac{\sum_{i=1}^{h} y^i \left(\prod_{j=1}^{n} A_j^i(x_j)\right)}{\sum_{i=1}^{h} \prod_{j=1}^{n} A_j^i(x_j)} = \omega^T \lambda(x), \quad (22)$$

where $A_j^i(x_j)$ is the membership function of the fuzzy variable xi, ω^T denotes the basis function vector of the fuzzy system, and $\lambda(x)$ is a fuzzy basis vector:

$$\lambda(x) = \begin{bmatrix} \lambda_1(x), & \lambda_2(x), & \ldots & \lambda_h(x) \end{bmatrix},$$

and $\lambda_i(x)$ defined as:

$$\lambda_i(x) = \frac{\prod_{j=1}^{n} A_j^i(x_j)}{\sum_{i=1}^{h} \left(\prod_{j=1}^{n} A_j^i(x_j)\right)}. \quad (23)$$

The functional form of fuzzy membership function for a fuzzy set $A_j^i(x_j)$ should be specified to develop the learning algorithms for these fuzzy systems. Take a Gaussian-shaped form as the membership function used in this study [29], [30]:

$$A_j^i(x_j) = \exp\left[-\frac{(x_j - p_j)^2}{2q_j^2}\right]. \quad (24)$$

According to the above formulas, the compound interference term $P_{n-\rho-1}$ can be expressed as:

$$P_{n-\rho-1} = \omega^T \lambda(x). \quad (25)$$

The optimal weight vector ω^* of the fuzzy system, for any given x in compact set Ω_ω, exists as [31]:

$$\omega^* = \arg\min_{\mu\in\Omega\omega}\left[\sup\left\|P_{n-\rho-1} - \omega^T\lambda(x)\right\|\right], \quad (26)$$

and

$$\Omega_\omega = \{\omega \,|\, \|\omega\| \le M\}, \quad (27)$$

where $M > 0$.

The fuzzy approximation error is defined as follow

$$P_{n-\rho-1} = \omega^T \varphi^* (x) + \varepsilon. \tag{28}$$

Adding fuzzy approximation and adaptive control law, set the control law is

$$U = U_m + U_1 + U_2, \tag{29}$$

where

$$U_1 = -\kappa_1 L_U L_C^{\rho-1}, \tag{30}$$

$$U_2 = -\kappa_2 L_U L_C^{\rho-1}. \tag{31}$$

It can be obtained from the above formulas

$$\begin{aligned} e^{(\rho)}(t) &= y^{(\rho)}(t) - Y_r^{(\rho)} \\ &= -KM_\rho + P_{n-\rho-1} - \kappa_1 - \kappa_2 \\ &= \begin{bmatrix} K_0 & K_1 & \cdots & K_{\rho-1} \end{bmatrix} \\ &\quad + \begin{bmatrix} e(t) & e^1(t) & \cdots & e^{(\rho-1)}(t) \end{bmatrix} \\ &\quad + P_{n-\rho-1} - \kappa_1 - \kappa_2, \\ e^{(\rho)}(t) &+ K_{\rho-1} e^{(\rho-1)}(t) + \cdots + K_0 e(t) \\ &\qquad - P_{n-\rho-1} + \kappa_1 + \kappa_2 = 0. \end{aligned}$$

Take $\widehat{e}$ as

$$\widehat{e} = \begin{bmatrix} e(t) & e^1(t) & \cdots & e^{(\rho-1)}(t) \end{bmatrix}^T.$$

Then the whole system error equation can be written as

$$\dot{\widehat{e}} = A\widehat{e} + B\left(\omega^T \lambda(x) + \varepsilon - v_r\right), \tag{32}$$

where

$$A = \begin{bmatrix} 0 & I_m & 0 & \cdots & 0 \\ 0 & 0 & I_m & \cdots & 0 \\ \vdots & \vdots & \vdots & & \vdots \\ 0 & 0 & 0 & \cdots & I_m \\ -K_0 & -K_1 & -K_2 & \cdots & -K_{\rho-1} \end{bmatrix}, \quad B = \begin{bmatrix} 0 \\ 0 \\ \vdots \\ 0 \\ I_m \end{bmatrix},$$

I_m is the m-dimensional unit matrix, $\tilde{\omega} = \omega^* - \omega$ is the weight error vector.

To overcome the impact of the approximation error on the system and improve the performance of the entire system, a robust compensation term should be introduced. Set the adaptive law as:

$$\kappa_2 = \alpha \tanh(\alpha\phi/\eta), \tag{33}$$

where, $\phi = B^T Q\hat{e}$, and η is design parameters for the controller.

The error vector and the Lyapunov function are defined as follows:

$$L(\Pi) = \Pi^T \tilde{Q} \Pi, \tag{34}$$

$$\Pi = \begin{bmatrix} \widehat{e}^T & \hat{\omega}^T & \tilde{\varphi} \end{bmatrix}^T \in D_\Pi, \tag{35}$$

where D is the domain of the augmented error, and $\bar{Q}$ is the weight matrix

$$\bar{Q} = \frac{1}{2} \begin{bmatrix} Q & 0 & 0 \\ 0 & \lambda_\omega^{-1} I_\omega & 0 \\ 0 & 0 & \lambda_\alpha^{-1} \end{bmatrix}, \tag{36}$$

and $Q = diag(Q_1, \cdots, Q_m)$, Q_m is design parameters, $\lambda_\alpha, \lambda_\omega > 0$.

The Lyapunov function defined by Equation (34) is derived from the system trajectory for time t.

$$\dot{L} = \frac{1}{2}\left(\dot{\widehat{e}}^T Q\widehat{e} + \widehat{e}^T Q\dot{\widehat{e}}\right) + \frac{1}{\lambda_\omega}\tilde{\omega}^T\dot{\tilde{\omega}} + \frac{1}{\lambda_\alpha}\tilde{\alpha}^T\dot{\tilde{\alpha}}, \tag{37}$$

$$\begin{aligned} \dot{L} &= \frac{1}{2}\dot{\widehat{e}}^T\left(QA + A^T Q\right)\widehat{e} + \widehat{e}^T QB\left(\tilde{\omega}^T\lambda(x) + \varepsilon - \kappa_2\right) \\ &\quad - \frac{1}{\lambda_\omega}\tilde{\omega}^T\dot{\tilde{\omega}} - \frac{1}{\lambda_\alpha}\tilde{\alpha}^T\dot{\tilde{\alpha}}, \end{aligned} \tag{38}$$

$$\begin{aligned} \dot{P} &\le -\frac{1}{2}\lambda_{\min}(Q)\left\|\widehat{e}\right\|^2 + \left\{\tilde{\omega}^T\lambda(x)s^T - \frac{1}{\lambda_\omega}\tilde{\omega}^T\dot{\tilde{\omega}}\right\} \\ &\quad + \left\{s^T(\varepsilon - v_r) - \frac{1}{\lambda_\alpha}\tilde{\alpha}^T\dot{\tilde{\alpha}}\right\} \\ &= -\frac{1}{2}\lambda_{\min}(Q)\left\|\widehat{e}\right\|^2 + \left\{\tilde{\omega}^T\lambda(x)s^T - \frac{1}{\lambda_\omega}\tilde{\omega}^T\dot{\tilde{\omega}}\right\} \\ &\quad + \left\{s^T(\varepsilon - \alpha\tanh(\alpha\phi/\eta)) - \frac{1}{\lambda_\alpha}\tilde{\alpha}^T\dot{\tilde{\alpha}}\right\}. \end{aligned}$$

The adaptive law can yield:

$$\begin{aligned} \dot{V} &\le -\frac{1}{2}\lambda_{\min}(Q)\left\|\widehat{e}\right\|^2 + K_\theta\tilde{\theta}^T\left(\theta^* - \tilde{\theta}\right) \\ &\qquad + \hat{\phi}\|s\| - s^T\hat{\lambda}\tanh\left(\hat{\lambda}\phi/\eta\right). \end{aligned} \tag{39}$$

Consider the following inequalities

$$\begin{aligned} \tilde{\theta}^T\left(\theta^* - \tilde{\theta}\right) &\le \left\|\tilde{\theta}\right\|\bar{\theta} - \left\|\tilde{\theta}\right\|^2 \le \frac{1}{2}\left(\left\|\tilde{\theta}\right\|^2 + \bar{\theta}^2\right) - \left\|\tilde{\theta}\right\|^2 \\ &= \frac{1}{2}\left(\bar{\theta}^2 - \left\|\tilde{\theta}\right\|^2\right), \\ \tilde{\varphi}^T(\varphi - \tilde{\varphi}) &\le \|\tilde{\varphi}\|\varphi - \|\tilde{\varphi}\|^2 \le \frac{1}{2}\left(\|\tilde{\varphi}\|^2 + \varphi^2\right) - \|\tilde{\varphi}\|^2 \\ &= \frac{1}{2}\left(\varphi^2 - \|\tilde{\varphi}\|^2\right), \end{aligned}$$

and

$$\begin{aligned} \dot{V} &\le -\frac{1}{2}\lambda_{\min}(Q)\left\|\widehat{e}\right\|^2 - \frac{K_\omega}{2}\left\|\tilde{\theta}\right\|^2 - \frac{K_\alpha}{2}\left\|\tilde{\phi}\right\|^2 + \frac{K_\omega}{2}\bar{\theta}^2 \\ &\quad + \frac{K_\alpha}{2}\phi^2 + m\xi\delta \\ &= -\frac{1}{2}\lambda_{\min}(Q)\left\|\widehat{e}\right\|^2 - \frac{K_\omega}{2}\|\tilde{\omega}\|^2 - \frac{K_\alpha}{2}\|\tilde{\alpha}\|^2 + c. \end{aligned} \tag{40}$$

When the following equation holds

$$\left\|\widehat{e}\right\| > \sqrt{\frac{2c_2}{\lambda_{\min}(Q)}}, \quad \|\tilde{\omega}\| > \sqrt{\frac{2c_2}{K_\omega}}, \quad \|\tilde{\alpha}\| > \sqrt{\frac{2c_2}{K_\alpha}},$$

according to the Lyapunov theory, the augmented error signal Π of the closed-loop system is finally bounded, and (40) can be written as:

$$\dot{V} \le -c_1 V + c_2.$$

Integrate the above formula from t to t_2

$$V(t) \le \frac{c_2}{c_1} + \left(V(t_0) - \frac{c_2}{c_1}\right)e^{-c_1(t-t_0)}. \tag{41}$$

Thus, for any given τ,

$$\tau > \sqrt{\frac{2c_2}{(\lambda_{\max}(P)\, c_1)}}.$$

There is a time $T > 0$, so that all of $t = t_0 + T$, and $\|\widehat{e}\| \leq \tau$.

The complex item in the rolling time domain expansion model of the system is improved by approximating with the FLS, and the robustness of the controller can be effectively improved by the adaptive law:

$$U = U_m + U_1 + U_2, \tag{42}$$

where

$$U_1 = -L_U L_C^{\rho-1} \omega^T \varphi(x),$$
$$U_2 = -L_U L_C^{\rho-1} \alpha \tanh(\alpha\phi/\eta).$$

IV. FRACTIONAL PID CONTROLLER

Satisfying the requirements of the system in a traditional controller is difficult due to the non-linearity of the active suspension hydraulic actuators. The fractional PID control, proposed by Podlubny [32], was developed from the traditional PID controller combined with the fractional calculus theory. Compared with previous ones, it is considered a better solution to the control problem of nonlinear systems and has been widely used in many applications [33], [34].

Many definitions of fractional calculus have been presented in previous studies. In the current study, we used the Grünwald–Letnikov definition in the proposes system [35]. The expression is given by

$${}_aD_t^{\alpha} f(t) = \lim_{h\to 0} h^{-\alpha} \sum_{j=0}^{\left[\frac{t-a}{h}\right]} (-1)^j \binom{\alpha}{j} f(t-jh). \tag{43}$$

The general transfer function of the fractional PID controller is given by [32]

$$G(s) = K_P + K_I s^{-\lambda} + K_D s^{\mu}, \tag{44}$$

where λ is the fractional calculus operator, α is the fractional order and $\lambda, \alpha > 0$.

Given that the fractional differential operator is a complex irrational function, it is usually solved by using an approximate algorithm. The Oustaloup approximate algorithm is a widely used algorithm [36] with the transfer function given by

$$G_f(s) = K \prod_{k=1}^{N} \frac{s + \omega_k'}{s + \omega_k}, \tag{45}$$

among them,

$$\omega_k' = \omega_b \left(\frac{\omega_h}{\omega_b}\right)^{\frac{k+N+\frac{1}{2}(1-\alpha)}{2N+1}}, \quad \omega_k = \omega_b \left(\frac{\omega_h}{\omega_b}\right)^{\frac{k+N+\frac{1}{2}(1+\alpha)}{2N+1}}, \quad K = \omega_h^{\alpha},$$

and ω_h is the upper cutoff frequency; ω_b is the lower cutoff frequency.

V. SIMULATION AND ANALYSIS

Compared with the traditional Sky-hook damper controlled active suspension, the active and passive suspension models are simulated. The simulation parameters are shown in Table 3 and the vertical acceleration, pitch angle acceleration, and roll angle acceleration of the vehicle body are shown below:

TABLE 3. Simulation parameters (i = 1, 2, 3, 4).

Parameter	Value	Parameter	Value
m	1500 Kg	ci	*1600 Ns/m*
mu	45 Kg	P_s	21 MPa
Jx	450 Kg·m^2	A_p	1.3×10^{-3} m^2
Jy	2100 Kg·m^2	τ	3.33×10^{-2} s
a	1.4 m	βe	750 MPa
b	1.7 m	V_t	3.50410^{-4} m^3
ki	14000 N/m	α	4.515×10^{13} N/m^5
kti	240000N/m		

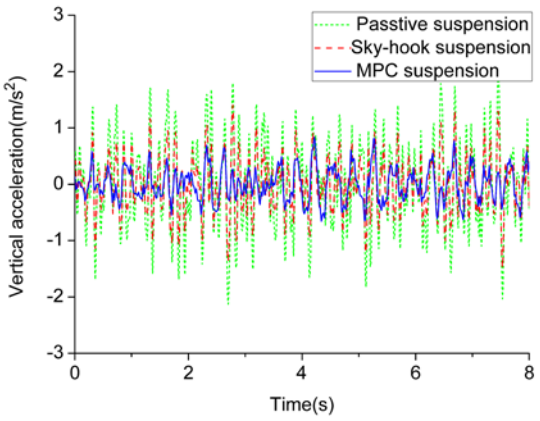

FIGURE 3. Vertical acceleration.

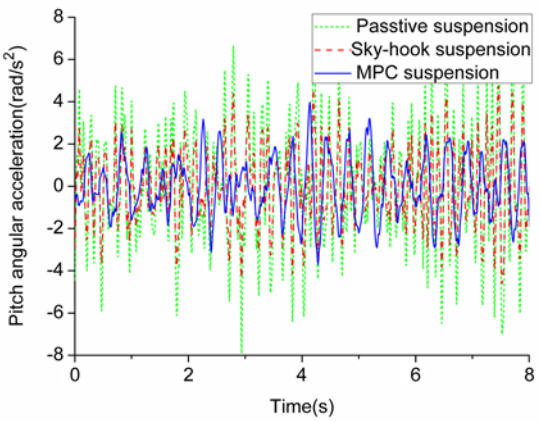

FIGURE 4. Pitch angle acceleration.

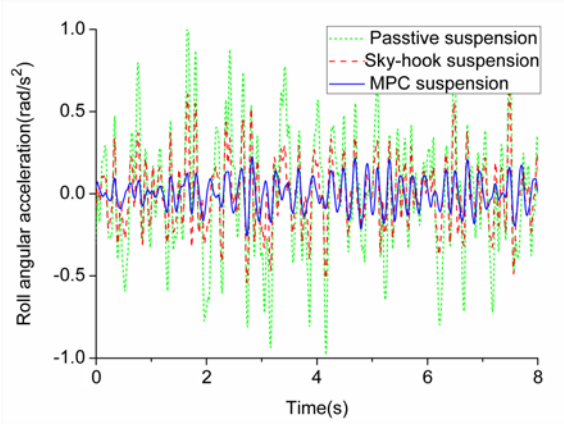

FIGURE 5. Roll angle acceleration.

Evidently, from the simulation diagrams and comparison with the passive suspension, the active suspension predictive control has a better performance. The body vibrations, such as vertical acceleration, pitch angle acceleration, and roll angle accelerations, were significantly reduced and effectively address the ride comfort and handling stability requirements of the vehicle (see Figs. 3–5).

VI. ROAD EXPERIMENTS AND RESULTS

Road experiments of the prototype vehicle were carried out to verify the accuracy and efficiency of the active suspension control algorithm. The main body of the prototype vehicle was assembled and constructed using the FAW Besturn car chassis, as shown in Fig. 6. It included the mechanical, hydraulic servo, and the electric control parts.

FIGURE 6. The prototype vehicle with active suspension.

The mechanical system comprised the passive suspension system, the steering system, the brake system, the vehicle frame, and the connecting parts. The hydraulic system consisted of a hydraulic pump station, an energy storage device, a hydraulic one-way valve, a relief valve, four electro-hydraulic servo valves, an electromagnetic directional valve, four hydraulic cylinders, and other auxiliary components. The electro-hydraulic servo valve controls the asymmetrical hydraulic cylinder to realize the active suspension function. The electronic control system mainly included a computer and sensors. Although the active suspension actuators can replace the spring and shock absorber in the passive suspension in a certain degree, but the contrast that considered the need to test for active suspension and passive suspension can realize the main function of the active and passive suspension switch connected in parallel through the electromagnetic reversing valve. This should be done without destroying the original passive suspension and active suspension hydraulic actuators.

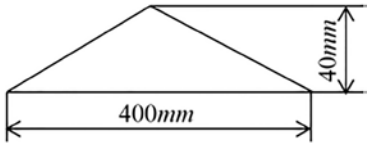

FIGURE 7. Test bump.

In the road experiments, the excitation input came in the form of a triangular bump, as shown in Fig. 7. Before the test started, the excitation bumps were placed in the middle of the test road, and the distance between the two pulse bumps was adjusted according to the wheelbase. The test vehicle passed through the bumps at uniform speed, the body posture was recorded when the front wheels of the car approached the bumps. The recording stopped when the car already passed by. The experimental data are shown in Fig. 8–10.

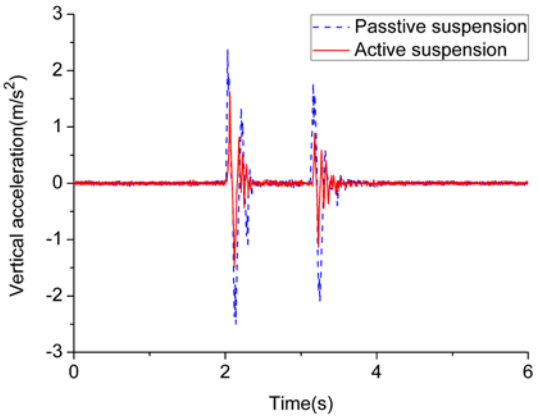

FIGURE 8. Vertical acceleration.

TABLE 4. Road experiment results compare.

	Active suspension	Passive suspension
vertical acceleration	1.602 m/s^2	2.375 m/s^2
pitch acceleration	1.882 rad/s^2	2.759 rad/s^2
roll acceleration	1.141 rad/s^2	2.090 rad/s^2

It can be seen from the data in Table 4 that the active suspension system with RMPC control in the pulse input test reduces the vertical acceleration peak by about 32.5%, the pitch acceleration peak by about 31.8% and the roll acceleration peak by about 45.4% compared to the passive

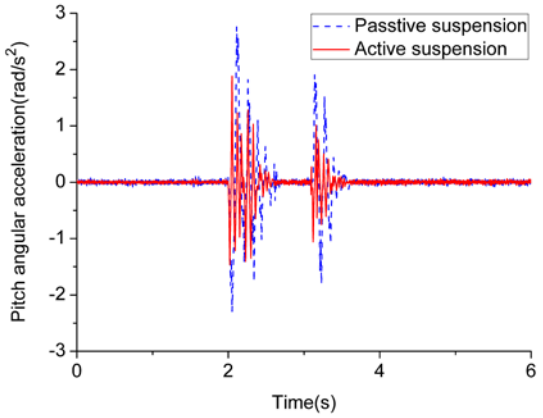

FIGURE 9. Pitch angle acceleration.

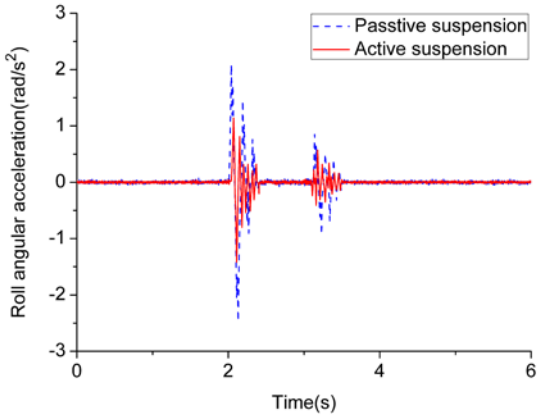

FIGURE 10. Roll angle acceleration.

suspension system. From the road experiments of the prototype vehicle, it can be seen that the active suspension system with RMPC has improved greatly in riding comfort compared to the passive suspension, and the validity and practicability of RMPC have also been verified.

VII. CONCLUSION

In this paper, the full-vehicle model is established for the EH servo active suspension and the model predictive controller is designed. The model predictive control based on the approximate expansion in the rolling time domain does not depend on the accuracy of the active suspension model. In the practical application process, the uncertainty factors for the model have improved. At the same time, in order to increase the practicability of the control system, the influence of active suspension hydraulic actuator is considered and effectively controlled by fractional PID controller. Compared with other suspension systems, the active suspension based on the model predictive control has obvious vibration reduction effect, such as vertical acceleration, pitch angle acceleration, and roll angle acceleration. This model can also effectively improve the vehicle performance to increase vehicle comfort and ensure vehicle handling stability. The effectiveness and practicality of the control system are further verified through the vehicle road experiments.

ACKNOWLEDGMENT

The authors also gratefully acknowledge the helpful comments and suggestions of the reviewers, which have improved the presentation.

REFERENCES

[1] M. Soleymani, M. Montazeri-Gh, and R. Amiryan, "Adaptive fuzzy controller for vehicle active suspension system based on traffic conditions," *Sci. Iranica*, vol. 19, no. 3, pp. 443–453, 2012.
[2] R.-J. Lian, "Enhanced adaptive self-organizing fuzzy sliding-mode controller for active suspension systems," *IEEE Trans. Ind. Electron.*, vol. 60, no. 3, pp. 958–968, Mar. 2013.
[3] W. Sun, Z. Zhao, and H. Gao, "Saturated adaptive robust control for active suspension systems," *IEEE Trans. Ind. Electron.*, vol. 60, no. 9, pp. 3889–3896, Sep. 2013.
[4] W. Sun, H. Pan, Y. Zhang, and H. Gao, "Multi-objective control for uncertain nonlinear active suspension systems," *Mechatronics*, vol. 24, no. 4, pp. 318–327, 2013.
[5] T. P. J. van der Sande, B. L. J. Gysen, I. J. M. Besselink, J. J. H. Paulides, E. A. Lomonova, and H. Nijmeijer, "Robust control of an electromagnetic active suspension system: Simulations and measurements," *Mechatronics*, vol. 23, no. 2, pp. 204–212, Aug. 2013.
[6] H. Li, J. Yu, C. Hilton, and H. Liu, "Adaptive sliding-mode control for nonlinear active suspension vehicle systems using T–S fuzzy approach," *IEEE Trans. Ind. Electron.*, vol. 60, no. 8, pp. 3328–3338, Aug. 2013.
[7] P. Brezas and M. C. Smith, "Linear quadratic optimal and risk-sensitive control for vehicle active suspensions," *IEEE Trans. Control Syst. Technol.*, vol. 22, no. 2, pp. 543–556, Mar. 2014.
[8] H. Pan, W. Sun, H. Gao, and J. Yu, "Finite-time stabilization for vehicle active suspension systems with hard constraints," *IEEE Trans. Intell. Transp. Syst.*, vol. 16, no. 5, pp. 2663–2672, Oct. 2015.
[9] V. S. Deshpande, P. D. Shendge, and S. B. Phadke, "Nonlinear control for dual objective active suspension systems," *IEEE Trans. Intell. Transp. Syst.*, vol. 18, no. 3, pp. 656–665, Mar. 2017.
[10] J. J. Rath, M. Defoort, H. R. Karimi, K. C. Veluvolu, "Output feedback active suspension control with higher order terminal sliding mode," *IEEE Trans. Ind. Electron.*, vol. 64, no. 2, pp. 1392–1403, Feb. 2017.
[11] S. J. Qin and T. A. Badgwell, "An overview of industrial model predictive control technology," *Control Eng. Pract.*, vol. 93, no. 7, pp. 232–256, Jan. 1997.
[12] J. Zhao, S. Zhou, and R. Zhou, "Distributed time-constrained guidance using nonlinear model predictive control," *Nonlinear Dyn.*, vol. 84, no. 3, pp. 1399–1416, 2016.
[13] J. Lopez-Sanz *et al.*, "Nonlinear model predictive control for thermal management in plug-in hybrid electric vehicles," *IEEE Trans. Veh. Technol.*, vol. 66, no. 5, pp. 3632–3644, May 2017.
[14] H.-T. Zhang, Y. Wu, D. He, and H. Zhao, "Model predictive control to mitigate chatters in milling processes with input constraints," *Int. J. Mach. Tools Manuf.*, vol. 91, pp. 54–61, Apr. 2015.
[15] T. Faulwasser and R. Findeisen, "Nonlinear model predictive control for constrained output path following," *IEEE Trans. Autom. Control*, vol. 61, no. 4, pp. 1026–1039, Apr. 2016.
[16] C. Gohrle, A. Schindler, A. Wagner, and O. Sawodny, "Design and vehicle implementation of preview active suspension controllers," *IEEE Trans. Control Syst. Technol.*, vol. 22, no. 3, pp. 1135–1142, May 2014.
[17] L. Cheng, W. Liu, Z.-G. Hou, J. Yu, and M. Tan, "Neural-network-based nonlinear model predictive control for piezoelectric actuators," *IEEE Trans. Ind. Electron.*, vol. 62, no. 12, pp. 7717–7727, Dec. 2015.
[18] Y. Hu, M. Z. Q. Chen, and Z. Hou, "Multiplexed model predictive control for active vehicle suspensions," *Int. J. Control*, vol. 88, no. 2, pp. 347–363, Apr. 2015.
[19] F. Schnelle and P. Eberhard, "Adaptive nonlinear model predictive control design of a flexible-link manipulator with uncertain parameters," *Acta Mech. Sinica*, vol. 33, no. 3, pp. 529–542, May 2017.
[20] M. Yamashita, K. Fujimori, K. Hayakawa, and H. Kimura, "Application of H_∞ control to active suspension systems," *Automatica*, vol. 30, no. 11, pp. 1717–1729, 1994.

[21] M. M. Fateh and S. S. Alavi, "Impedance control of an active suspension system," *Mechatronics*, vol. 19, no. 1, pp. 134–140, 2009.
[22] A. G. Alleyne and R. Liu, "Systematic control of a class of nonlinear systems with application to electrohydraulic cylinder pressure control," *IEEE Trans. Control Syst. Technol.*, vol. 8, no. 4, pp. 623–634, Jul. 2000.
[23] W. Sun, H. Gao, and B. Yao, "Adaptive robust vibration control of full-car active suspensions with electrohydraulic actuators," *IEEE Trans. Control Syst. Technol.*, vol. 21, no. 6, pp. 2417–2422, Nov. 2013.
[24] W.-H. Chen, D. J. Ballance, and P. J. Gawthrop, "Optimal control of nonlinear systems: A predictive control approach," *Automatica*, vol. 39, no. 4, pp. 633–641, 2003.
[25] W. H. Chen, "Predictive control of general nonlinear systems using approximation," *IEE Proc-Control Theory Appl.*, vol. 151, no. 2, pp. 137–144, 2004.
[26] M. R. Abedi and F. Tahami, "A nonlinear model predictive controller design for Sheppard–Taylor based PFC rectifier," in *Proc. 35th Annu. Conf. IEEE Ind. Electron.*, Nov. 2009, pp. 1403–1408.
[27] L.-X. Wang, "Stable adaptive fuzzy control of nonlinear systems," *IEEE Trans. Fuzzy Syst.*, vol. 1, no. 2, pp. 146–155, May 1993.
[28] S. Tong and H.-X. Li, "Fuzzy adaptive sliding-mode control for MIMO nonlinear systems," *IEEE Trans. Fuzzy Syst.*, vol. 11, no. 3, pp. 354–360, Jun. 2003.
[29] X. Zhao, P. Shi, and X. Zheng, "Fuzzy adaptive control design and discretization for a class of nonlinear uncertain systems," *IEEE Trans. Cybern.*, vol. 46, no. 6, pp. 1476–1483, Jun. 2016.
[30] Y. Li, S. Tong, and T. Li, "Hybrid fuzzy adaptive output feedback control design for uncertain MIMO nonlinear systems with time-varying delays and input saturation," *IEEE Trans. Fuzzy Syst.*, vol. 24, no. 4, pp. 841–853, Aug. 2016.
[31] Y.-J. Liu and W. Wang, "Adaptive fuzzy control for a class of uncertain nonaffine nonlinear systems," *Inf. Sci.*, vol. 177, no. 18, pp. 3901–3917, 2007.
[32] I. Podlubny, "Fractional-order systems and $PI^{\lambda}D^{\mu}$ controllers," *IEEE Trans. Autom. Control*, vol. 44, no. 1, pp. 208–214, Jan. 1999.
[33] X. Liu, "Optimization design on fractional order PID controller based on adaptive particle swarm optimization algorithm," *Nonlinear Dyn.*, vol. 84, no. 1, pp. 379–386, 2016.
[34] X. Dong, D. Zhao, B. Yang, and C. Han, "Fractional-order control of active suspension actuator based on parallel adaptive clonal selection algorithm," *J. Mech. Sci. Technol.*, vol. 30, no. 6, pp. 2769–2781, 2016.
[35] P. Shah and S. Agashe, "Review of fractional PID controller," *Mechatronics*, vol. 38, pp. 29–41, Sep. 2016.
[36] A. Oustaloup, F. Levron, B. Mathieu, and F. M. Nanot, "Frequency-band complex noninteger differentiator: Characterization and synthesis," *IEEE Trans. Circuits Syst. I, Fundam. Theory Appl.*, vol. 47, no. 1, pp. 25–39, Jan. 2000.

DAZHUANG WANG received the B.Eng. degree from the Changchun University of Science and Technology in 2012. He is currently pursuing the Ph.D. degree with the School of Mechanical Science and Engineering, Jilin University. His research interests are active suspension control, electrohydraulic servo control, and mechanical system dynamics.

DINGXUAN ZHAO is currently a Distinguished Professor of the Chang Jiang Scholars Program and also a Professor with the School of Mechanical Engineering, Yanshan University. His main research interests are engineering robotics, dynamics, and simulation of complex mechanical systems.

MINGDE GONG is currently a Professor with the School of Mechanical Engineering, Yanshan University. His main research interests are engineering robotics, robot teleoperation technologies, and transmission and control of construction machinery.

BIN YANG is currently a Senior Engineer with Jilin University. His main research interests are engineering robotics, active suspension control, electrohydraulic servo control, and transmission and control of construction machinery.